Hindawi Publishing Corporation
Journal of Nanomaterials
Volume 2015, Article ID 807394, 10 pages
http://dx.doi.org/10.1155/2015/807394

Research Article

Facile Synthesis and Characterization of N-Doped TiO_2 Photocatalyst and Its Visible-Light Activity for Photo-Oxidation of Ethylene

Yu-Hao Lin,[1] Chih-Huang Weng,[2] Arun Lal Srivastav,[3] Yao-Tung Lin,[3] and Jing-Hua Tzeng[3]

[1]*Centre for Environmental Restoration and Disaster Reduction, National Chung Hsing University, 250 Kuo Kuang Road, Taichung 40227, Taiwan*
[2]*Department of Civil and Ecological Engineering, I-Shou University, Kaohsiung City 84008, Taiwan*
[3]*Department of Soil and Environmental Sciences, National Chung Hsing University, 250 Kuo Kuang Road, Taichung 40227, Taiwan*

Correspondence should be addressed to Yao-Tung Lin; yaotung@nchu.edu.tw

Received 25 August 2014; Accepted 10 December 2014

Academic Editor: Yuekun Lai

A facile wet chemical method was adopted for preparing highly photoactive nitrogen doped TiO_2 (N-TiO_2) powders with visible responsive capability, which could be achieved by the hydrolysis of titanium isopropoxide (TTIP) in the ammonium hydroxide precursor solution in various concentrations and then calcined at different temperatures. The N-TiO_2 powders were characterized, and the photocatalytic activity was evaluated for the photocatalytic oxidation of ethylene gas under visible light irradiation to optimize the synthesizing conditions of N-TiO_2 catalyst. The N-TiO_2 photocatalytic powders were calcined in a range of temperatures from 300 to 600°C and obviously found to have greater photocatalytic activities than commercial TiO_2 P25. The strong absorption in the visible light region could be ascribed to good crystallization and adapted sinter temperature of as prepared sample. XPS test demonstrated that the N was doped into TiO_2 lattice and made an interstitial formation (Ti-O-N), and N doping also retarded the phase transformation from anatase to rutile as well. The N-TiO_2 catalyst prepared with 150 mL ammonium hydroxide added and calcined at 500°C showed the best photocatalytic activity. The experimental results also proved the enhanced photoactivity of N-TiO_2 material depends on the synthesizing conditions.

1. Introduction

Recently, the nanomaterial, such as nanoiron, titanium dioxide photocatalysts (TiO_2), has applied for groundwater remediation, degradation of hazardous materials, and environment cleanup [1–3]. However, the wide band gap of TiO_2 for anatase crystal structure requires UV light and occupied less than 10% energy in solar spectrum for the excitation of electron-hole pairs [4], which restricts the application of TiO_2 because of low photo quantum efficiency.

Various metals such as Ag have been doped into the TiO_2 lattice to shift its absorption from UV to visible light, and doping improved their photocatalytic activities [5]. In addition, literatures also fabricated the nanotube array or hybrid structures of element-doped-TiO_2 to enhance the photocatalytic activity [6, 7]. However, none of them gave satisfactory results due to their thermally instability and increased carrier trapping [8]. Relatively, the doping of anion on TiO_2 such as nitrogen and carbon element doped and codoped has considerable effect on increasing its photocatalytic activity [9–14], in which, the nitrogen seems to be the most effective dopant due to its similar size to oxygen and metastable defect complex, as well as small ionization energy [15], and N-doped TiO_2 (N-TiO_2) has an advantage on photocatalytic activity [16, 17]. Hence, literatures focused on discussing the structure of N-TiO_2 using the X-ray photoelectron spectroscopy (XPS), electron spin resonance, or X-ray absorption near edge structure. Some reports claim that the band gap of the N-TiO_2 is reduced due to a rigid valence band shift upon doping [18], others attributed the observed

absorption of visible light by N-TiO_2 to the excitation of electrons from localized N-impurity states in the band-gap [8, 19]. In general, the change in banding structure of N-TiO_2 was attributed to the N interstitial doping, N substitution, and O vacancy [20–22]. However, till now the structure of N-TiO_2 is still under debate. The preparatory methods and conditions such as nitrogen precursor and sintering temperature may considerably affect the nitrogen state in the doped TiO_2 [19, 23]. But, only few systematic discussions have been found regarding the dominated factor ratio of N to Ti and calcination temperature for the activity of N-TiO_2, simultaneously.

In other words, it is necessary to understand the chemical fine-tuning and further optimization of the visible-light photocatalytic activity of N-TiO_2. The goal of this study is (1) to develop a simple method for the synthesis of N-TiO_2 nanomaterials using facie method at various conditions of nitrogen precursor amounts and composite calcination temperatures, (2) characterization of N-TiO_2 composite materials, (3) carried out the photocatalytic activity of as prepared N-TiO_2 under visible light.

Ethylene is a plant hormone that controls many plant responses, and its higher concentration can affect the food and horticultural product industry [24], safe handling, and the parent compound of important environmental contaminants, and the photocatalytic activity for the degradation was quite different from that of volatile chlorinated organic compounds such as trichloroethylene [25]. Therefore, batch experiments were conducted for the removal of ethylene to evaluate the N-TiO_2 photoactivity under visible light irradiation and have also been compared with that of commercial photocatalysts Degussa P25. Materials characterizations have been performed through specific surface area analysis, X-ray diffraction (XRD), scanning electron microscope (SEM), electron Spectroscopy for Chemical Analysis (ESCA), and diffuse reflectance ultraviolet-visible absorption spectra (DRS UV-vis).

2. Materials and Methods

2.1. Chemicals and Synthesis of N-TiO_2 Composite. All the chemicals were used as procured without further purification. Commercial photocatalyst P25 was purchased from Degussa. Ammonium hydroxide (NH_4OH, 33 wt%), titanium tetraisopropoxide (TTIP), and absolute ethanol (99.8%) were procured from J. T. Baker. Synthesis procedure of N-TiO_2 composite was modified as reported in literatures [16, 26], and ammonium hydroxide was chosen as a nitrogen precursor. Different amounts of ammonium hydroxide (0–200 mL) and DI water (200–0 mL) were mixed with absolute ethanol (200 mL) in a flask, and then a 400 mL ammonia solution (concentration 0–8.4 M) was obtained. The 10 ml TTIP was added dropwise into the ammonia solution and stirred vigorously for 4 h at 4°C in a water bath. After that the hydrolysis and condensation reaction was kept on stirring for 24 h at room temperature, and then the sol-gel solutions stood to 24 h in aged conditions. The ensuing colloid was then centrifuged and washed thoroughly with distilled water to remove the residual reactants. The final precipitate was dried at 105°C overnight in air and calcined at various temperatures for 5 h to obtain the final N-TiO_2 composite. The synthesized N-TiO_2 composites were labeled as N_xT_y, where x and y represent the amount (mL) of ammonium hydroxide added during the synthesis procedure and calcinations temperature (unit is 100°C per scale), respectively. For example, the $N_{150}T_5$ catalyst indicates the addition of 150 mL ammonium hydroxide during the sol-gel procedure of amorphous N-TiO_2 catalyst, followed by its calcination at 500°C temperature. Pure TiO_2 catalyst was named as $N_{00}T_y$ (x means "zero"), and there was not any addition of ammonium hydroxide during synthesis procedure, such that N_0T_3 refers to the pure TiO_2 catalyst which was calcined at 300°C temperature.

2.2. Characterization of Composite. The composite was characterized by means of XRD, DRS UV-vis, XPS, and specific surface area. XPS were recorded on an ESCA spectrometer (ULVAC-PHI, PHI 5000, Japan) operated at 150 W and were used to investigate the surface properties in the valence band of the composite. The shift of the binding energy due to relative surface charging was corrected using the C 1s as an internal standard. The optical absorption responses of composite were obtained from the pressed disk composite using UV-vis (Hitachi, U-3900H, Japan) equipped with an integrated sphere, and $BaSO_4$ was used as a reference. Specific surface areas of samples were obtained by the Brunauer-Emmett-Teller (BET) method using nitrogen adsorption apparatus (Micromeritics ASAP 2020, USA). Samples were degassed at 150°C for 2 h prior to the measurements. The crystal phases of the composites were analyzed by XRD (PANalytical X'Pert Pro MRD, USA) with Cu-Ka radiation and diffraction angle range of 2θ which is 20° to 80°. The crystal size was determined according to Scherrer's equation and fraction of anatase phase in the mixture was calculated by formula proposed by Spurr [27].

2.3. Photocatalytic Activity of N-TiO_2. During this study, removal ethylene was studied in batch experiment modes to evaluate the photocatalytic activity of N-TiO_2 samples as well as commercial photocatalyst P25. All the powders (0.5 g) were coated onto the flask bottle (catalyst film was kept at 1 mg/cm^2) and caped with sleeve stoppers. The constant ethylene was injected into the flask to get initial ethylene concentration (about 140 or 85 ppmv in different test); a 150 μL aliquot regularly was withdrawn and injected into gas chromatograph equipment equipped with flame ionization detector (PerkinElmer Clarus 500, USA) to analyze the ethylene concentration. The visible illumination was provided by six three-colored fluorescent lamps (March T5-8W/865), located above the flasks equipped with a filter to cut the UV light region. The visible irradiance 610 nm was determined by detector (international light SED005) and about 0.62 mW/cm^2 at the bottom of flask.

3. Result and Discussions

3.1. BET, XRD, and SEM Analysis. The characteristics of composites including surface area, anatase phases, and crystallite size are summarized in Table 1 and Figure 1, in which, the

Table 1: Characteristics and rate constant of N-doped TiO_2 prepared at various N/Ti ratio and calcinations temperature.

Sample	BET				XRD		SEM	UV-vis		Activity
	Specific surface area	Pore size	Pore volume	Adsorption type[a]	Phase content[b]	Crystalline size[c]	Size	Band gap[d]		Rate constant
	m^2/g	nm	cm^3/g	cm^3/g	A/R/B (%)	nm	nm	Eg1 (eV)	Eg2 (eV)	$\times 10^{-2}\ h^{-1}$
$N_{00}T_2$	258.9	3.4	0.28	IV	78/00/22	14	—	—	—	—
$N_{00}T_3$	144.7	4.8	0.24	IV	79/00/22	17	—	2.03	2.99	—
$N_{00}T_4$	70.1	5.3	0.25	IV	82/00/18	24	—	—	3.04	—
$N_{00}T_5$	65.8	6.2	0.17	IV	86/00/14	55	22	—	3.05	0.63*
$N_{00}T_6$	19.5	9.6	0.08	IV	92/08/00	113	—	—	2.91	—
$N_{00}T_7$	0.5	18.3	0.01	V	28/72/00	138	—	—	2.87	—
$N_{00}T_8$	0.2	25.9	0.00	V	06/94/00	155	—	—	—	—
$N_{50}T_3$	144.8	4.8	0.24	IV	100/00/0	31	—	2.51	3.18	1.72#
$N_{100}T_3$	231.7	3.9	0.28	IV	100/00/0	28	—	2.51	3.06	1.09#
$N_{150}T_3$	186.1	4.0	0.27	IV	100/00/0	27	—	2.46	3.12	1.93# 0.87*
$N_{200}T_3$	260.4	3.5	0.27	IV	100/00/0	25	—	2.52	3.05	1.29*
$N_{150}T_2$	319.9	3.2	0.22	IV	—	—[e]	—	—	—	—
$N_{150}T_4$	61.0	6.6	0.16	IV	100/00/0	36	—	2.38	3.10	1.50*
$N_{150}T_5$	45.3	6.9	0.13	IV	100/00/0	37	21.3	2.39	3.13	1.76*
$N_{150}T_6$	34.2	9.3	0.11	IV	100/00/0	62	—	—	3.01	1.54*
$N_{150}T_7$	0.8	29.5	0.03	V	78/22/00	108	—	—	2.92	0.01*
$N_{150}T_8$	1.6	39.7	0.04	V	58/42/00	113	—	—	2.92	0.00*
P25	51.2	18.7	0.25	IV	82/18/00	62	—		3.04	0.47*

[a]Adsorption isotherm type and hysteresis loop were based on the IUPAC manual; [b]A, R, and B denote anatase, rutile, and brookite, respectively; [c]from XRD data using Scherer formula; [d]the band gap is determined by the plot of $(\alpha h\nu)^{1/2}$ versus photon energy, as shown in Figure 4; [e]no obvious characteristic pattern of crystal to calculate the size; *experimental conditions: reaction temp. = 20°C, R.H. = 63%, $[C_2H_4]_{initial}$ = 140 ppmv, light intensity = 0.62 mW/cm^2; #experimental conditions: reaction temp. = 20°C, R.H. = 53%, $[C_2H_4]_{initial}$ = 85 ppmv, light intensity = 0.62 mW/cm^2.

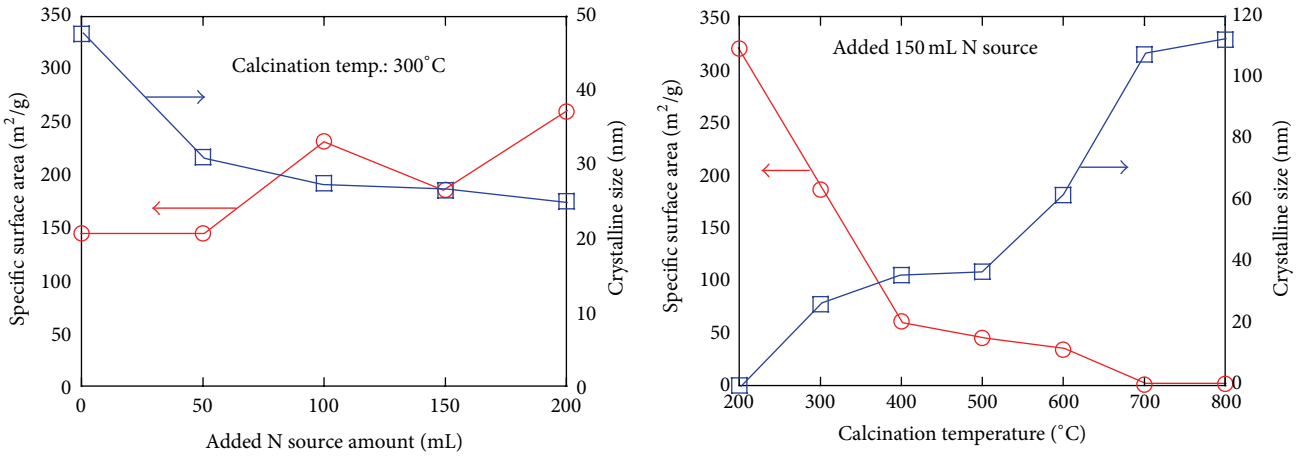

FIGURE 1: The specific surface area of N-TiO_2 samples as a function of (a) the various ammonium hydroxide amounts added and (b) calcinations temperature.

crystallite size and phase content of sample is calculated using the Scherrer equation from XRD peak position and full width half maximum [27]. Comparing Figure 1(a) with Figure 1(b), the unobvious change in the BET surface area and crystalline size of samples were observed after the addition of N precursor amounts. However, the clear changes in composites at different calcination temperatures depicted that the dominant factor for surface area and crystalline size of catalysts are calcination temperature, not the addition of N amounts. The pore size and pore volume of composite relative to surface area decreased with the increase of the calcination temperature, and this result is attributed to the pores collapsed and bigger crystallites aggregation of catalyst [28].

The XRD patterns of N-TiO_2 samples in different conditions are shown in Figure 2. The diffraction peaks marked with letters "A" and "R" on the figure corresponds to the anatase and rutile phase, respectively. In Figure 2(a), the major peak of 2 theta at about 25.5° corresponding to crystal plane (101) of anatase, which became thinner and the relative intensity was increased with calcination temperature. Such stronger crystalline flair of catalyst would enhance its photoactivity. The XRD patterns of N-TiO_2 synthesized with different nitrogen precursors presented in Figure 2(b) have also shown the similar results. It was also depicted that the nitrogen precursor amount did not significantly affect the N-TiO_2 crystal phase and crystal size.

The N-TiO_2 catalyst ($N_{150}T_3$) shows great effect on the photoactivity and also prevents the conversion of N-doped amount into nitrogen gas during calcination process. This sample synthesized with 150 mL N precursor was tested to investigate the effects of calcination temperature and the result is presented in Figure 2(c).

In Figures 2(a) and 2(c), the anatase phase on pure and N-doped TiO_2 sample started to appear at 200°C and 300°C calcination temperatures, respectively. The phase transformation from anatase to rutile was observed after the 600°C and 700°C calcination temperatures. This result can be implied that the nitrogen-doped catalyst retarded the phase transformation [10]. Such higher thermal stability could elevate the anatase crystallinity and promoted the photo-induced charge separation and transportation [29]. The interesting brookite phase was only observed in pure TiO_2 (see Figure 2(a)) and disappeared as the beginning of rutile phase, and further the inhibited form of the brookite phase in the N-TiO_2 was implied (Figure 2(c)), since the addition of nitrogen in N-TiO_2 catalyst. Figures 2(b) and 2(c) showed that the N-doped TiO_2 samples had typical peaks of polycrystalline anatase structure and rutile without any detectable dopant related peaks, such as TiN, which was possibly due to the movement of dopant ions either into interstitial positions or substitutional sites of the TiO_2 structure or ion concentration, was detected to be too low [30].

The morphology and particle size of the N-TiO_2 ($N_{150}T_5$) and pure TiO_2 ($N_{00}T_5$) samples can be obtained from an examination of the SEM image (Figure 3). Single particle in agglomerates in both of them exhibited uniform spherical shape; the size was in range from 20 to 25 nm and a narrow size distribution appeared. Both of these sizes were slightly smaller than the crystallite sizes determined from the XRD in Figure 1(b). The results of similar size and morphology also indicated that the N precursor did not have significant effect on the particle size and shape of TiO_2 catalyst.

3.2. DRS UV-Vis and ESCA. In this study, the N-TiO_2 powders sintered below 600°C, all exhibited a pale yellow color which suggests its ability to absorb light in the visible region [31]. However, Qiu and Burda infer that the obtained UV-vis spectra that localized defect states may also play a role in providing visible light activity [32]. Optical absorption spectra of the N-TiO_2 and Degussa P25 samples are shown in Figure 4, and the absorption at wavelengths shorter than 400 nm can be assigned to the intrinsic band gap absorption of TiO_2. A significant shift of the absorption edge to a lower energy in the visible-light region was observed for N-doped TiO_2. This result indicates that band-gap narrowing has successfully been achieved by the doping of N into the TiO_2 lattice, presumably due to the modification of the band structure

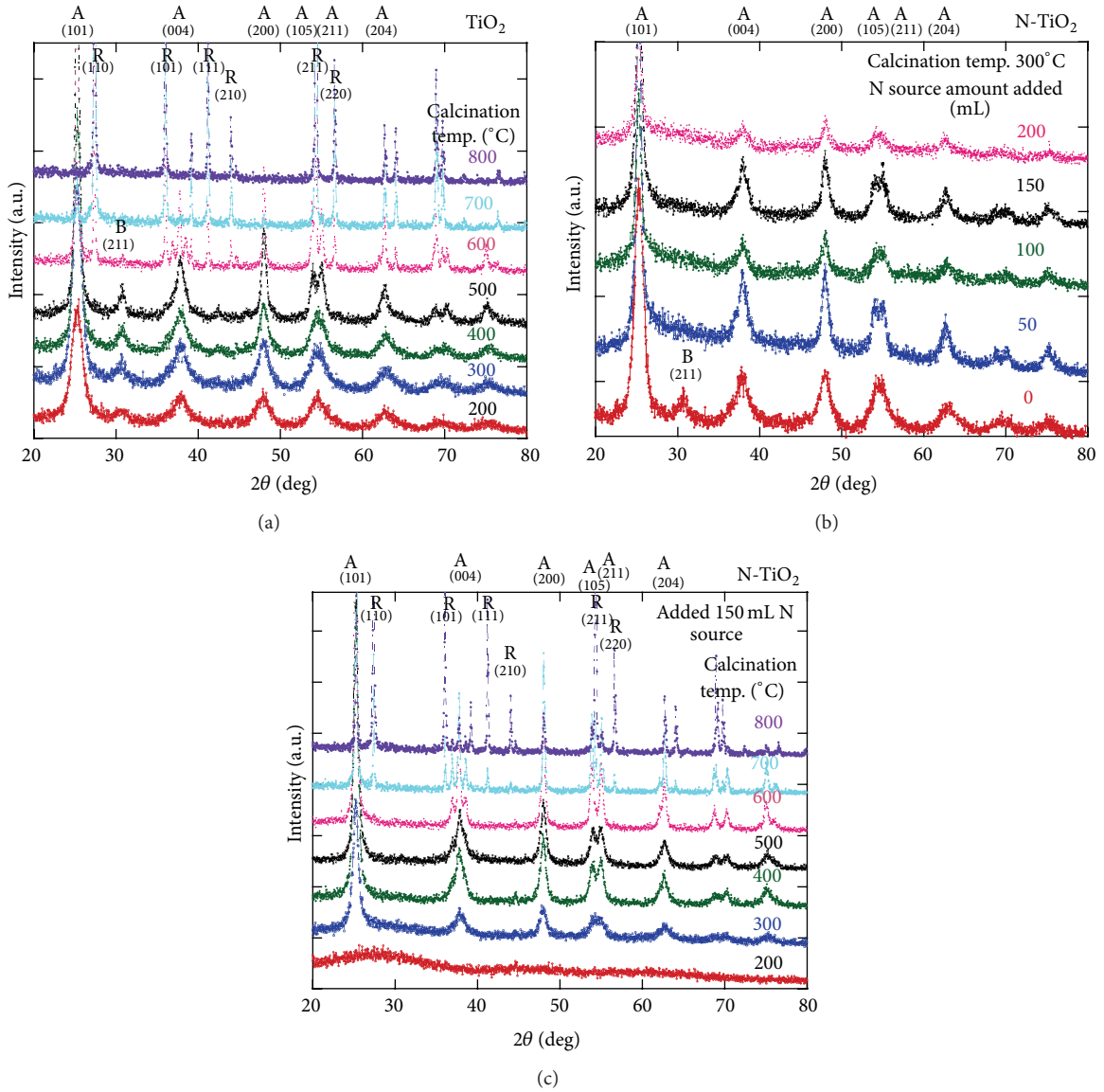

FIGURE 2: XRD pattern of (a) pure TiO_2 calcined at different temperature, (b) N-TiO_2 samples synthesized in different loading of ammonium hydroxide amounts, and (c) N-TiO_2 samples calcined at different temperature.

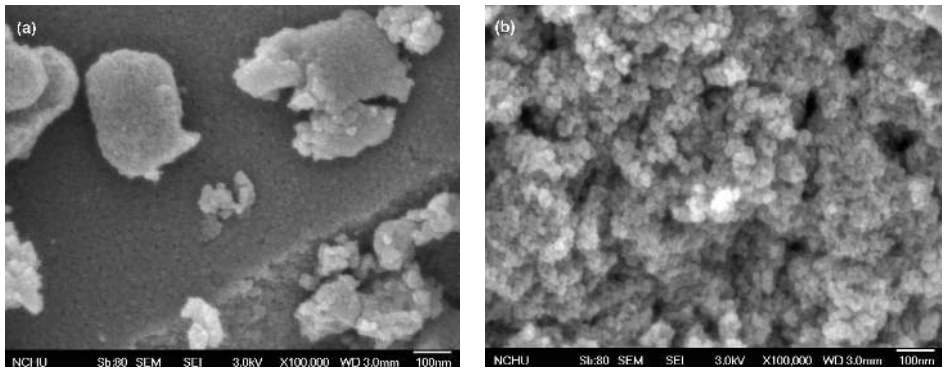

FIGURE 3: SEM images of (a) pure TiO_2 and (b) N-TiO_2 catalyst.

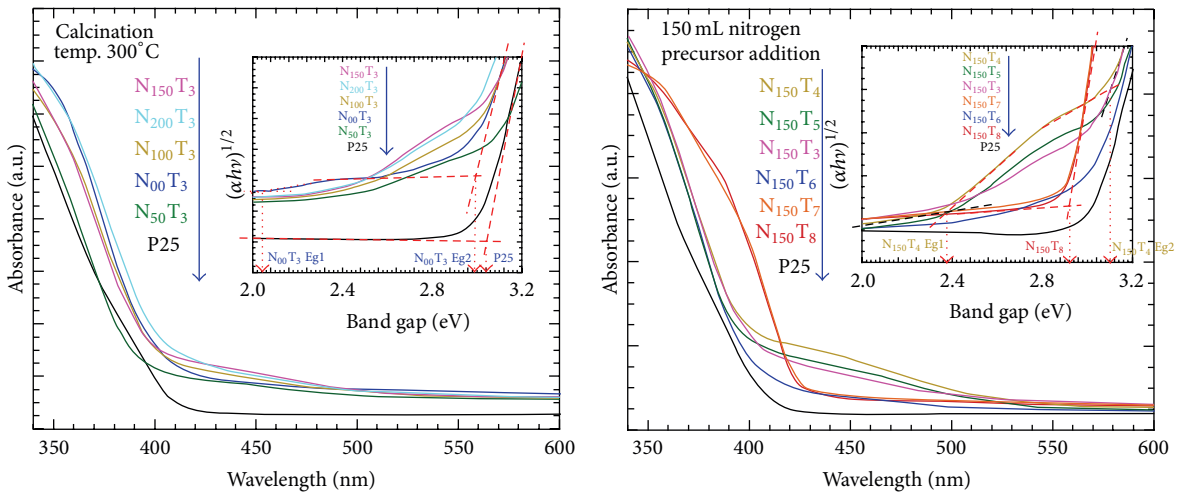

(a) (b)

FIGURE 4: The UV-vis adoption pattern of N-TiO_2 (a) prepared with various ammonium hydroxide amount added and (b) calcined at different temperature.

[33]. The absorption spectra of the N-doped TiO_2 samples show a stronger absorption than undoped TiO_2 as well as P25 in the UV-vis light region and a red shift in the band gap transition except $N_{50}T_3$ sample. The red shift is ascribed possibly to the oxygen vacancy [34] or the fact that N doping can narrow the band gap of the TiO_2 [35, 36]. Generally, the photocatalytic activity is proportional to the photo numbers absorbed by photocatalyst per second and the efficiency of the band gap transition [28], the N doping expand the wavelength response range of TiO_2 into the visible region and also increased the number of photo-generated electrons and holes to enhance the photocatalytic performance of N-TiO_2. The enhanced activity in N-TiO_2 catalysts also was demonstrated in Figure 6. Figure 4(a) revealed that the absorbance increases with increasing added nitrogen precursor amounts of N-TiO_2 synthesized condition.

Unfortunately, such absorbance is not proportional to its photoactivity. Further, the UV-vis absorbance spectra of appropriate samples with different calcined temperature are shown in Figure 4(b). The absorbance of all N-TiO_2 samples in the visible region is higher than that of P25 and may be ascribed to the fact that the narrowing of band gap as well as localized defect resulted from N doping and calcination. Higher than 700°C calcination, the N-TiO_2 powders show a significant red shift in the band gap transition due to the formation of rutile phase and growth of TiO_2 crystallite. However, interestingly, amorphous $N_{150}T_2$ powders also showed a greatest red shift. As the calcination temperature increased from 300°C to 600°C, the intensive absorption of $N_{150}T_4$, $N_{150}T_3$, and $N_{150}T_5$ were observed in the visible region between 400 and 500 nm, which is the typical absorption feature of nitrogen doped TiO_2 [10], whereas it was not observed on $N_{150}T_6$ sample even if $N_{150}T_6$ appeared better photoactivity than $N_{150}T_3$. However, the aforementioned result could not possibly provide a definite relation between absorbance and photoactivity of as-prepared sample, which is due to that the absorption features in the visible range originated from color centers through doping processes or posttreatments rather than by narrowing of the band gap [32, 37]. Literature also reports the intensive absorption of ion doped TiO_2 that can be assigned to oxygen vacancies produced by thermal treatment, which form localization levels within the band gap [34]. Moreover, the origin of visible light absorption originated from N and O vacancies suggested that the N dopants can only affect the absorption below 500 nm wavelength, while the O vacancies are responsible for the induced absorption at wavelengths above 500 nm [38].

ESCA analyses of N 1s and Ti 2p were performed on pure TiO_2, P25, and N-TiO_2 catalysts and results are shown in Figure 5. In Figure 5(a), the binding energy (BE) peaks corresponding to N 1s core-levels for N-TiO_2 samples prepared with various amounts of N precursor and calcined at 300°C are observed one major peak at 398–402 eV. However, sometime the binding energy observed at 400 eV is ascribed to N atoms which are incorporated into the TiO_2 lattice as N_2 molecules [33]. Saha and Tompkins investigated the N 1s ESCA spectra during the oxidation of TiN and assigned the peaks as atomic β-N (396 eV) and molecularly chemisorbed γ-N2 (400 eV and 402 eV) [31]. Those different N 1s spectral features are still debated and dependent on different preparation methods and conditions [35]. Further, the Ti $2p_{1/2}$ and Ti $2p_{3/2}$ spin-orbital splitting photoelectrons for anatase TiO_2 were located at binding energies of about 464.0 and 458.2 eV, respectively, which were assigned to the presence of typical Ti^{4+}. Same Ti 2p peaks are located at same binding energy and distribution (Figure 5(b)), because the N precursor amount was not a dominating factor in the electronic structure of N-TiO_2, although the different activity of N-TiO_2 synthesized in N precursor amount is shown in Figure 6(a).

The content of nitrogen were maintained in all the composites smaller than 1% and found decreased with increasing calcination temperature as shown in Figure 5(c), which may be due to the replacement of N in the matrix by O and

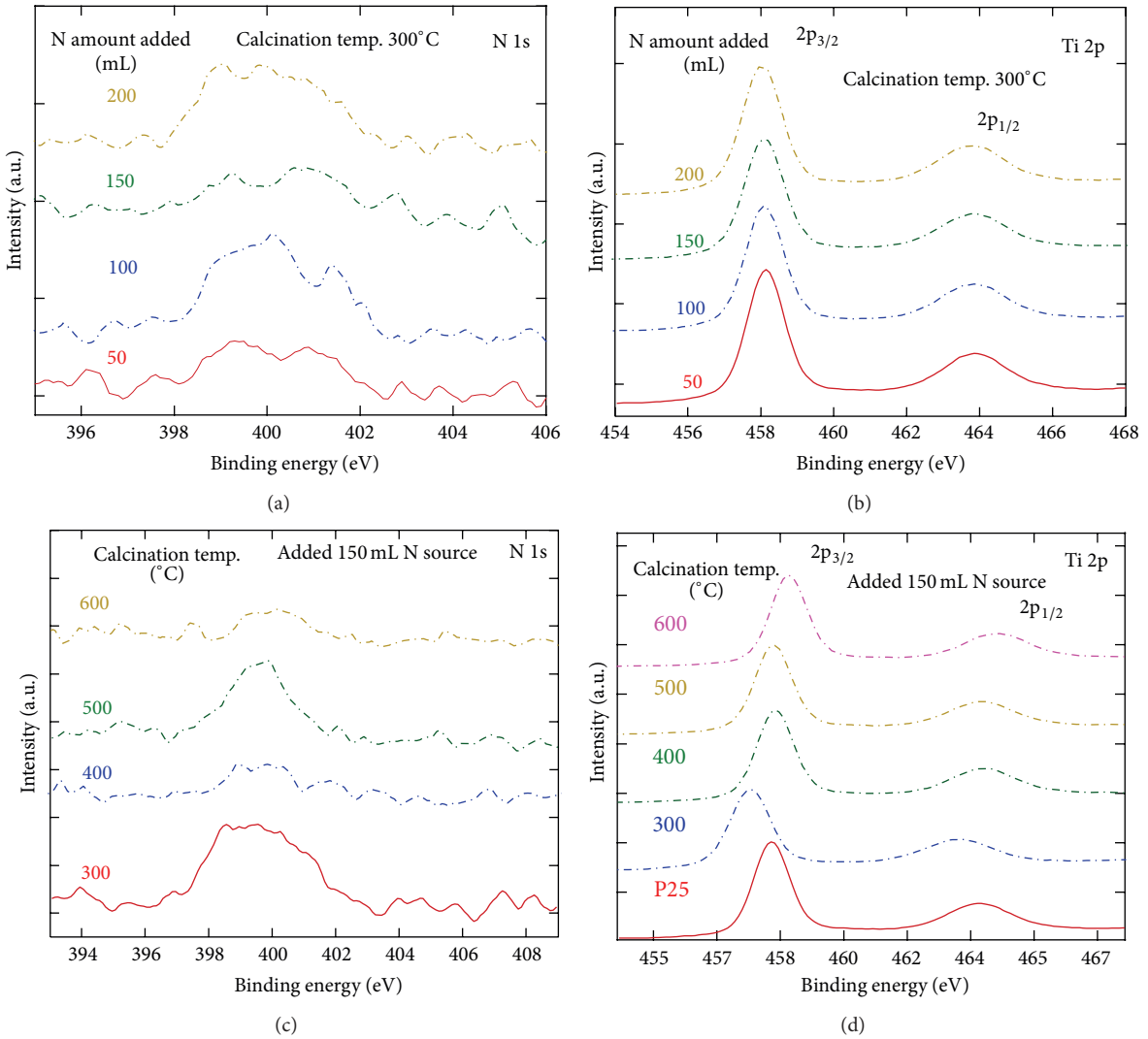

FIGURE 5: The XPS spectra for N-TiO_2 samples, ((a) and (c)) N 1s and ((b) and (d)) Ti 2p.

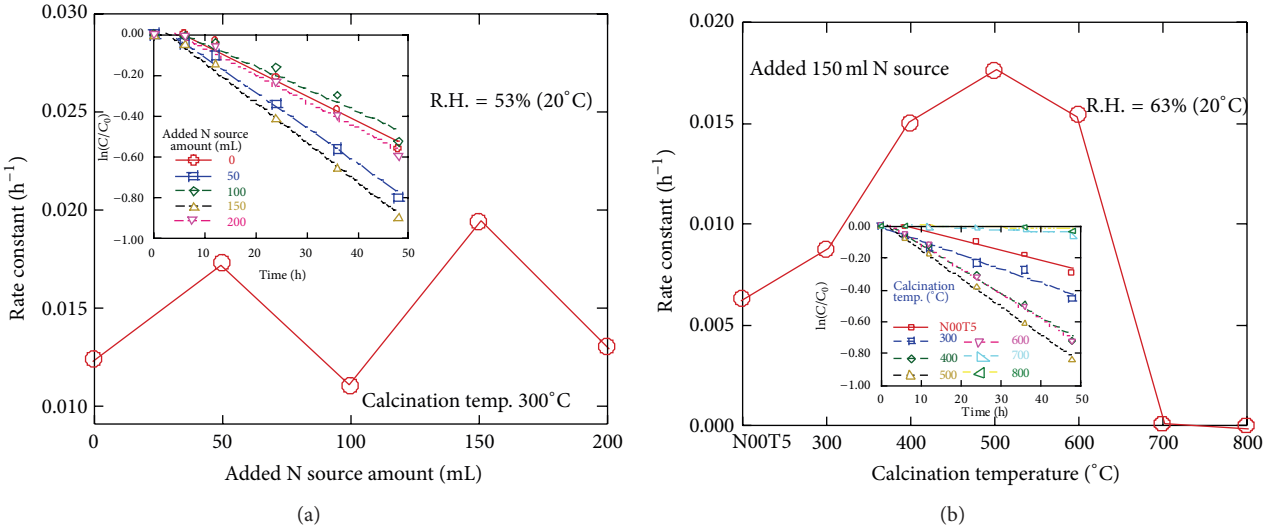

FIGURE 6: Photocatalytic reaction of N-TiO_2 samples as a function of (a) the various ammonium hydroxide amount added and (b) the various calcination temperature.

transform to nitride result in lower N concentrations [32]. Literature reports that the N dopant was adsorbed NO or bond to oxygen vacancy site in interstitial formation (Ti-O-N), especially at such low N doping concentrations [39]. The N 1s peaks also shifted towards higher binding energy with increasing calcination temperature level and appeared as different distribution. However, high sintering temperature can also cause the loss of dopants from N-TiO_2 catalyst. Therefore, an appropriate sintering temperature would be more important to the activity of N-doped TiO_2 [32]. At the same time, in Figure 5(d), the Ti 2p peaks undergone a shift towards higher binding energy with increasing calcination temperatures. This indicates the lowering of electronic density around the central Ti ion by introducing more O next to Ti [32]. The above mentioned binding energy shift pointed out that the calcination temperature may be a dominating factor in the electronic structure of N-TiO_2, and this is found consistent with XRD and BET analyses, and thus the calcination temperature would be key factor for the characteristics of N-TiO_2 based on synthesized method of this study.

3.3. Photoactivity of N-TiO_2 under Visible Light Illumination. Figure 6 shows the photocatalytic performances for ethylene removal over the various N-TiO_2 and pure TiO_2 in batch reactions under the visible light irradiation. The rate of photocatalytic oxidation has been described by a pseudo-first-order equation, as presented in (1) [24] and the rate constant values are given in Table 1. Consider

$$\ln\left(\frac{C_0}{C_t}\right) = -kt, \tag{1}$$

where C_0 is the initial concentration of ethylene, C_t is the ethylene at time t, and k is the apparent pseudo first photocatalytic oxidation rate constant. Examination of (1) suggests that the apparent pseudo first photocatalytic oxidation rate constant k can be determined experimentally from a plot of $\ln(C_0/C_t)$ versus time, which has a slope of $-k$. All the photocatalytic oxidation rate constants (k) of catalysts are summarized in Table 1. Figure 6(a) shows the effect of N-TiO_2 synthesized at different nitrogen precursor with 300°C calcination temperature, and the order of the reaction rates (Table 1) was $N_{150}T_3$, $N_{50}T_3$, $N_{200}T_3$, $N_{00}T_3$, and $N_{100}T_3$. Then, the N-TiO_2 catalyst was synthesized at 150 mL nitrogen precursor and sintered from 300°C to 800°C temperatures to investigate the effects of sintering temperature on N-TiO_2 photoactivity. In Figure 6(b), the activity of $N_{00}T_5$ (Pure TiO_2 sintered at 500°C temperature) was found better than commercial TiO_2 P25 under visible light irradiation due to the transfer of electron and hole between two phases (mix phase of anatase with few fraction of brookite) which is ascribed to the oxygen vacancy resulted from the calcination at 500°C [40].

Moreover, the optimized $N_{150}T_5$ photocatalyst has shown better ethylene degradation than undoped $N_{00}T_5$ and others. Based on the experimental results, the nitrogen doping would improve the photoactivity of undoped TiO_2 under visible light irradiation. Both $N_{150}T_7$ and $N_{150}T_8$ showed less photoactivity due to the existence of rutile phases and the tiny BET surface area as shown in Figure 1(b). However, the largest specific surface area of $N_{150}T_3$ should have theoretically better photoactivity for the removal of ethylene due to the abundance of active sites. More effectiveness of $N_{150}T_5$ was also observed for visible region of solar illumination and there are some other facts that may affect photoactivity of TiO_2 under visible illumination such as O vacancy resulted from calcination and N impurity acted as light sensitization [41, 42]. We have found that not only is the N-TiO_2 sample oxygen-deficient but also it involves a small amount of N-doped. N doping in TiO_2 was in interstitial formation (Ti-O-N) and that function retarded the reoxidation of oxygen deficient TiO_2, which is essentially indispensable for visible light sensitization [36].

4. Conclusions

N-TiO_2 nanocatalysts can be developed directly by so-gel method under the conditions: 150 mL ammonium hydroxide precursor added and 500°C calcination temperature. The ethylene removal efficiency was dependent on the optimal contents of nitrogen precursor, surface area, and oxygen vacancy and good crystallization resulted from the adapted calcination temperatures [32, 43]. The N-TiO_2 powders showed a stronger absorption in the visible light region from 400 to 500 nm wavelength, which was possibly due to narrow band gap by mixing of N 2p states with O 2p states on the top of the valence band or a creation of N-induced mid-gap level. Other more intensive absorption in the visible light region longer than 500 nm wavelength is ascribed to oxygen vacancy resulted from the calcination and N doping. The N-doping wet-method has an advantage on photocatalytic activity as compared to metal ion doping (thermally instability). In addition, the doped TiO_2 enhanced the photoactivity may be further investigated in depth [32], such as use of first principle calculations, origin of the enhanced visible light absorption in N-doped anatase TiO_2 [44], or approaches to combine TiO_2 with another mineral such as schorl.

Conflict of Interests

The authors declare that there is no conflict of interests regarding the publication of this paper.

Acknowledgment

This research was financially supported by the National Science Council of Taiwan ROC under Grants nos. NSC-100-2221-E-005-007 and NSC-101-2120-M-005-001.

References

[1] Y.-H. Lin, H.-H. Tseng, M.-Y. Wey, and M.-D. Lin, "Characteristics, morphology, and stabilization mechanism of PAA250K-stabilized bimetal nanoparticles," *Colloids and Surfaces A: Physicochemical and Engineering Aspects*, vol. 349, no. 1–3, pp. 137–144, 2009.

[2] Y.-H. Lin, H.-H. Tseng, M.-Y. Wey, and M.-D. Lin, "Characteristics of two types of stabilized nano zero-valent iron and transport in porous media," *Science of the Total Environment*, vol. 408, no. 10, pp. 2260–2267, 2010.

[3] Y.-T. Lin, C.-H. Weng, and T. W. Tzeng, "Photocatalysis and catalytic properties of nano-sized N-TiO_2 Catalyst synthesized by Sol-gel methods," *Journal of Advanced Oxidation Technologies*, vol. 13, no. 3, pp. 297–304, 2010.

[4] T. C. Jagadale, S. P. Takale, R. S. Sonawane et al., "N-doped TiO_2 nanoparticle based visible light photocatalyst by modified peroxide sol-gel method," *Journal of Physical Chemistry C*, vol. 112, no. 37, pp. 14595–14602, 2008.

[5] L. Sun, J. Li, C. Wang et al., "Ultrasound aided photochemical synthesis of Ag loaded TiO_2 nanotube arrays to enhance photocatalytic activity," *Journal of Hazardous Materials*, vol. 171, no. 1–3, pp. 1045–1050, 2009.

[6] Y.-K. Lai, J.-Y. Huang, H.-F. Zhang et al., "Nitrogen-doped TiO_2 nanotube array films with enhanced photocatalytic activity under various light sources," *Journal of Hazardous Materials*, vol. 184, no. 1–3, pp. 855–863, 2010.

[7] Y. Tang, P. Wee, Y. Lai et al., "Hierarchical TiO_2 nanoflakes and nanoparticles hybrid structure for improved photocatalytic activity," *The Journal of Physical Chemistry C*, vol. 116, no. 4, pp. 2772–2780, 2012.

[8] M. Sathish, B. Viswanathan, R. P. Viswanath, and C. S. Gopinath, "Synthesis, characterization, electronic structure, and photocatalytic activity of nitrogen-doped TiO_2 nanocatalyst," *Chemistry of Materials*, vol. 17, no. 25, pp. 6349–6353, 2005.

[9] B. F. Abramović, D. V. Šojić, V. B. Anderluh, N. D. Abazović, and M. I. Čomor, "Nitrogen-doped TiO_2 suspensions in photocatalytic degradation of mecoprop and (4-chloro-2-methylphenoxy)acetic acid herbicides using various light sources," *Desalination*, vol. 244, no. 1–3, pp. 293–302, 2009.

[10] Y. Ma, J. Zhang, B. Tian, F. Chen, and L. Wang, "Synthesis and characterization of thermally stable Sm,N co-doped TiO_2 with highly visible light activity," *Journal of Hazardous Materials*, vol. 182, no. 1–3, pp. 386–393, 2010.

[11] S.-I. In, P. C. K. Vesborg, B. L. Abrams, Y. Hou, and I. Chorkendorff, "A comparative study of two techniques for determining photocatalytic activity of nitrogen doped TiO_2 nanotubes under visible light irradiation: photocatalytic reduction of dye and photocatalytic oxidation of organic molecules," *Journal of Photochemistry and Photobiology A: Chemistry*, vol. 222, no. 1, pp. 258–262, 2011.

[12] Z. Xie, Y. Zhang, X. Liu et al., "Visible light photoelectrochemical properties of N-doped TiO_2-nanorod arrays from TiN," *Journal of Nanomaterials*, vol. 2013, Article ID 930950, 8 pages, 2013.

[13] Y.-T. Lin, C.-H. Weng, Y.-H. Lin, C.-C. Shiesh, and F.-Y. Chen, "Effect of C content and calcination temperature on the photocatalytic activity of C-doped TiO_2 catalyst," *Separation and Purification Technology*, vol. 116, pp. 114–123, 2013.

[14] X. Cheng, H. Liu, Q. Chen, J. Li, and P. Wang, "Construction of N, S codoped TiO_2 NCs decorated TiO_2 nano-tube array photoelectrode and its enhanced visible light photocatalytic mechanism," *Electrochimica Acta*, vol. 103, pp. 134–142, 2013.

[15] C. H. Park, S. B. Zhang, and S.-H. Wei, "Origin of p-type doping difficulty in ZnO: the impurity perspective," *Physical Review B*, vol. 66, no. 7, Article ID 073202, 2002.

[16] S. Sato, R. Nakamura, and S. Abe, "Visible-light sensitization of TiO_2 photocatalysts by wet-method N doping," *Applied Catalysis A: General*, vol. 284, no. 1-2, pp. 131–137, 2005.

[17] Y.-T. Lin, C.-H. Weng, H.-J. Hsu, Y.-H. Lin, and C.-C. Shiesh, "The synergistic effect of nitrogen dopant and calcination temperature on the visible-light-induced photoactivity of N-doped TiO_2," *International Journal of Photoenergy*, vol. 2013, Article ID 268723, 13 pages, 2013.

[18] R. Asahi, T. Morikawa, T. Ohwaki, K. Aoki, and Y. Taga, "Visible-light photocatalysis in nitrogen-doped titanium oxides," *Science*, vol. 293, no. 5528, pp. 269–271, 2001.

[19] C. Di Valentin, E. Finazzi, G. Pacchioni et al., "N-doped TiO_2: theory and experiment," *Chemical Physics*, vol. 339, no. 1–3, pp. 44–56, 2007.

[20] O. Diwald, T. L. Thompson, T. Zubkov, E. G. Goralski, S. D. Walck, and J. T. Yates Jr., "Photochemical activity of nitrogen-doped rutile TiO_2 (110) in visible light," *Journal of Physical Chemistry B*, vol. 108, no. 19, pp. 6004–6008, 2004.

[21] X. Chen and C. Burda, "Photoelectron spectroscopic investigation of nitrogen-doped titania nanoparticles," *Journal of Physical Chemistry B*, vol. 108, no. 40, pp. 15446–15449, 2004.

[22] S. Hu, A. Wang, X. Li, and H. Löwe, "Hydrothermal synthesis of well-dispersed ultrafine N-doped TiO_2 nanoparticles with enhanced photocatalytic activity under visible light," *Journal of Physics and Chemistry of Solids*, vol. 71, no. 3, pp. 156–162, 2010.

[23] Y. Zhao, X. Qiu, and C. Burda, "The effects of sintering on the photocatalytic activity of N-Doped TiO_2 nanoparticles," *Chemistry of Materials*, vol. 20, no. 8, pp. 2629–2636, 2008.

[24] S. Y. Ye, Q. M. Tian, X. L. Song, and S. C. Luo, "Photoelectrocatalytic degradation of ethylene by a combination of TiO_2 and activated carbon felts," *Journal of Photochemistry and Photobiology A: Chemistry*, vol. 208, no. 1, pp. 27–35, 2010.

[25] S. Yamazaki, S. Tanaka, and H. Tsukamoto, "Kinetic studies of oxidation of ethylene over a TiO_2 photocatalyst," *Journal of Photochemistry and Photobiology A: Chemistry*, vol. 121, no. 1, pp. 55–61, 1999.

[26] S. Sato, "Photocatalytic activity of NO_x-doped TiO_2 in the visible light region," *Chemical Physics Letters*, vol. 123, no. 1-2, pp. 126–128, 1986.

[27] R. A. Spurr, "Quantitative analysis of anatase-rutile mixtures with an X-ray diffractometer," *Analytical Chemistry*, vol. 29, no. 5, pp. 760–762, 1957.

[28] J. Yu, M. Zhou, B. Cheng, and X. Zhao, "Preparation, characterization and photocatalytic activity of in situ N,S-codoped TiO_2 powders," *Journal of Molecular Catalysis A: Chemical*, vol. 246, no. 1-2, pp. 176–184, 2006.

[29] Y. Luan, L. Jing, M. Xie et al., "Synthesis of efficient N-containing TiO_2 photocatalysts with high anatase thermal stability and the effects of the nitrogen residue on the photoinduced charge separation," *Physical Chemistry Chemical Physics*, vol. 14, no. 4, pp. 1352–1359, 2012.

[30] N. D. Abazović, A. Montone, L. Mirenghi, I. A. Janković, and M. I. Čomor, "TiO_2 doped with nitrogen: synthesis and characterization," *Journal of Nanoscience and Nanotechnology*, vol. 8, no. 2, pp. 613–618, 2008.

[31] N. C. Saha and H. G. Tompkins, "Titanium nitride oxidation chemistry: an x-ray photoelectron spectroscopy study," *Journal of Applied Physics*, vol. 72, no. 7, pp. 3072–3079, 1992.

[32] X. Qiu and C. Burda, "Chemically synthesized nitrogen-doped metal oxide nanoparticles," *Chemical Physics*, vol. 339, no. 1–3, pp. 1–10, 2007.

[33] T. Morikawa, R. Asahi, T. Ohwaki, K. Aoki, and Y. Taga, "Band-gap narrowing of titanium dioxide by nitrogen doping," *Japanese Journal of Applied Physics*, vol. 40, no. 6, pp. L561–L563, 2001.

[34] I. Nakamura, N. Negishi, S. Kutsuna, T. Ihara, S. Sugihara, and K. Takeuchi, "Role of oxygen vacancy in the plasma-treated TiO_2 photocatalyst with visible light activity for NO removal," *Journal of Molecular Catalysis A: Chemical*, vol. 161, no. 1-2, pp. 205–212, 2000.

[35] Z. Wu, F. Dong, W. Zhao, and S. Guo, "Visible light induced electron transfer process over nitrogen doped TiO_2 nanocrystals prepared by oxidation of titanium nitride," *Journal of Hazardous Materials*, vol. 157, no. 1, pp. 57–63, 2008.

[36] T. Ihara, M. Miyoshi, Y. Iriyama, O. Matsumoto, and S. Sugihara, "Visible-light-active titanium oxide photocatalyst realized by an oxygen-deficient structure and by nitrogen doping," *Applied Catalysis B: Environmental*, vol. 42, no. 4, pp. 403–409, 2003.

[37] N. Serpone, "Is the band gap of pristine TiO_2 narrowed by anion- and cation-doping of titanium dioxide in second-generation photocatalysts?" *The Journal of Physical Chemistry B*, vol. 110, no. 48, pp. 24287–24293, 2006.

[38] Z. Lin, A. Orlov, R. M. Lambert, and M. C. Payne, "New insights into the origin of visible light photocatalytic activity of nitrogen-doped and oxygen-deficient anatase TiO_2," *Journal of Physical Chemistry B*, vol. 109, no. 44, pp. 20948–20952, 2005.

[39] A. Nambu, J. Graciani, J. A. Rodriguez, Q. Wu, E. Fujita, and J. F. Sanz, "N doping of $TiO_2(110)$: photoemission and density-functional studies," *Journal of Chemical Physics*, vol. 125, no. 9, Article ID 094706, 2006.

[40] T. Ozawa, M. Iwasaki, H. Tada, T. Akita, K. Tanaka, and S. Ito, "Low-temperature synthesis of anatase-brookite composite nanocrystals: the junction effect on photocatalytic activity," *Journal of Colloid and Interface Science*, vol. 281, no. 2, pp. 510–513, 2005.

[41] M. Batzill, E. H. Morales, and U. Diebold, "Influence of nitrogen doping on the defect formation and surface properties of TiO_2 rutile and anatase," *Physical Review Letters*, vol. 96, no. 2, Article ID 026103, 2006.

[42] H. Chen, A. Nambu, W. Wen et al., "Reaction of NH_3 with titania: N-doping of the oxide and TiN formation," *The Journal of Physical Chemistry C*, vol. 111, no. 3, pp. 1366–1372, 2007.

[43] H. Fu, L. Zhang, S. Zhang, Y. Zhu, and J. Zhao, "Electron spin resonance spin-trapping detection of radical intermediates in N-doped TiO_2-assisted photodegradation of 4-chlorophenol," *Journal of Physical Chemistry B*, vol. 110, no. 7, pp. 3061–3065, 2006.

[44] M. Harb, P. Sautet, and P. Raybaud, "Origin of the enhanced visible-light absorption in N-doped bulk anatase TiO_2 from first-principles calculations," *The Journal of Physical Chemistry C*, vol. 115, no. 39, pp. 19394–19404, 2011.